

REPORT DOCUMENTATION PAGE

The public reporting burden for this collection of information is estimated to average 1 hour searching existing data sources, gathering and maintaining the data needed, and completing regarding this burden estimate or any other aspect of this collection of information, including Defense, Washington Headquarters Services, Directorate for Information Operations and F 1204, Arlington, VA 22202-4302. Respondents should be aware that notwithstanding any penalty for failing to comply with a collection of information if it does not display a currently valid control number.

AFRL-SR-AR-TR-05-

0475

ctions,
ments
ent of
Suite
o any

PLEASE DO NOT RETURN YOUR FORM TO THE ABOVE ADDRESS.

1. REPORT DATE (DD-MM-YYYYJ) 10-31-2005		2. REPORT TYPE final		3. DATES COVERED (From - To) 8/1/2002 - 7/30/2005	
4. TITLE AND SUBTITLE THE ROLE OF MITOCHONDRIA IN THE DETECTION OF INFRARED LIGHT SOURCES BY MAMMALIAN CELLS.				5a. CONTRACT NUMBER	
6. AUTHOR(S) Guenter Albrecht-Buehler, Ph.D, Robert Laughlin Rea Professor of Cell Biology, Department of Cell and Molecular Biology				5b. GRANT NUMBER F49620-02-1-0395	
7. PERFORMING ORGANIZATION NAME(S) AND ADDRESSE(S) Northwestern University Medical School 303 E. Chicago Ave., CHICAGO, IL 60611T Tel.: (312)-503-4261, Fax: 312-503-7912, e-mail: g-buehler@northwestern.edu				5c. PROGRAM ELEMENT NUMBER	
9. SPONSORING/MONITORING AGENCY NAME(S) AND ADDRESSE(S)				5d. PROJECT NUMBER	
12. DISTRIBUTION/AVAILABILITY STATEMENT public availability				5e. TASK NUMBER	
13. SUPPLEMENTARY NOTES Approved for Public Release Distribution Unlimited				5f. WORK UNIT NUMBER	
				8. PERFORMING ORGANIZATION REPORT NUMBER	
				10. SPONSOR/MONITOR'S ACRONYMS)	
				11. SPONSOR/MONITOR'S REPORT NUMBERS)	
14. ABSTRACT With permission of the Program Director, Dr. Hugh DeLong and in cooperation with the DARPA programs "Persistence in Combat (PIC) " and "Regenesis" (Program Director: Cmdr. Dr.Kurt Henry) the emphasis was shifted to the detection and recording of near-infrared emissions of mammalian cells. The results warranted an immediate re-emphasis on the biological role of near-infrared detection by mammalian cells. During the past grant period we developed a novel and quantitative method to link the near-infrared light scattering of the cells to the distance from which a cell aggregate recruits its members. In short, it measures how far cell can 'see' each other in the following way. Each cellular aggregate forming on an isotropic, solid surface defines a circular area that marks the initial locations of its cells. The article uses a novel assay to measure the radius R_a of this circle ('range of aggregation') and shows in the case of 3T3 cells that it relates directly to the intensity I_{sc} of their near-infrared light scattering. The results suggest that cells detect distant others by their scattered near-infrared light.					
15. SUBJECT TERMS					
16. SECURITY CLASSIFICATION OF:					
a. REPORT	b. ABSTRACT	c. THIS PAGE	17. LIMITATION OF ABSTRACTS	18 NUMBER OF PAGES	19a. NAME OF RESPONSIBLE PERSON
U	U	U	UU		19b. TELEPHONE NUMBER (Include area code)

FINAL REPORT

1. PERIOD COVERED: August 1, 2002 – July 30, 2005

2. TITLE OF PROPOSAL: THE ROLE OF MITOCHONDRIA IN THE DETECTION OF INFRARED LIGHT SOURCES BY MAMMALIAN CELLS.

3. CONTRACT OR GRANT NUMBER: F49620-02-1-0395

4. NAME OF INSTITUTION: Northwestern University, Chicago

5. AUTHORS) OF REPORT: Guenter Albrecht-Buehler, Ph.D

Robert Laughlin Rea Professor of Cell Biology

Department of Cell and Molecular Biology

303 E. Chicago Ave. CHICAGO, IL 60611T

Tel.: (312)-503-4261

Fax: 312-503-7912

e-mail: g-buehler@northwestern.edu

6. LIST OF MANUSCRIPTS SUBMITTED OR PUBLISHED:

Albrecht-Buehler, G. A long-range attraction between aggregating 3T3 cells mediated by near-infrared light scattering (2005) Proc. Natl. Acad. Sci. USA 102:5050-5055

7. SCIENTIFIC PERSONNEL SUPPORTED BY THIS GRANT

Guenter Albrecht-Buehler, Ph.D.,

P.I.

8. BRIEF OUTLINE OF RESEARCH FINDINGS

a. Status of effort

With permission of the Program Director, Dr. Hugh DeLong and in cooperation with the DARPA programs "Persistence in Combat (PIC)" and "RegenesiS" (Program Director: Cmdr. Dr. Kurt Henry) the emphasis was shifted to the detection and recording of near-infrared emissions of mammalian cells. The results warranted an immediate re-emphasis on the biological role of near-infrared detection by mammalian cells. During the past grant period we developed a novel and quantitative method to link the near-infrared light scattering of the cells to the distance from which a cell aggregate recruits its members. In short, it measures how far cell can 'see' each other.

b. Accomplishments

Summary

Each cellular aggregate forming on an isotropic, solid surface defines a circular area that marks the initial locations of its cells. The article uses a novel assay to measure the radius R_a of this circle ('range of aggregation') and shows in the case of 3T3 cells that it relates directly to the intensity I_{sc} of their near-infrared light scattering. The results suggest that cells detect distant others by their scattered near-infrared light.

Introduction

The earlier finding that 3T3 cells detected pulsating near-infrared light signals (1) begged the questions of (a) their natural sources and (b) their biological function. Subsequent experiments with BHK cells growing on opposite faces of a thin film of glass (2) showed that they reacted to other cells across the glass barrier with no other means of detection than near-infrared light.

No artificial light sources were involved in these experiments. Keeping in mind that even 'dark' culture incubators emit thermal (black body) radiation corresponding to their temperature of 37°C, the results left us essentially with two possibilities for the natural light sources. Either the cells scattered the near-infrared portion of the blackbody radiation or they actively radiated such light.

In spite of efforts to count single photons with highly sensitive photomultiplier equipment and to apply advanced data analytical methods such as Fourier analysis and wavelet analysis no near-infrared light radiation of small groups of 3T3 cells could be detected. Instead, only the faint and noisy scattering of the ambient thermal radiation by the cells could be recorded (unpublished data). It appeared, therefore, that cells must rely on the naturally scattered near-infrared light of other cells to detect them.

Consequently, one should be able to change the behavior of cells by mere changes of their light scattering. In order to test this prediction a variant 3T3 cell line was isolated that formed a specific reticular

20051110 021

pattern in culture ('3T3_x cells') and investigated the role of cellular light scattering on their specific culture morphology.

In order to manipulate their light scattering the cells were allowed to ingest particles in the range of 0.5 – 3 [μm] diameter which mimicked the geometric properties of the perinuclear granules (see Fig.1a) but scattered considerably more light. Latex and synthetic diamond particles were used as they were inert and could be expected to have no chemical effect on the genome, membrane and cytoplasm of the internalizing cells. Cells loaded with these particles ('hyper-scattering cells') were then tested for their aggregation abilities. The test employed a novel assay that facilitated the detection of aggregates by restricting the cells to an essentially in one-dimensional space.

The present article reports that the light scattering of hyper-scattering cells related directly to the distance R_a at which aggregating cells come together.

The biological significance of the aggregation behavior of cells has been established over many decades by studies of cellular self-sorting, i.e. the homotypic aggregation of cells out of an initially random mixture of two or more different cell types in organ culture. Since Holtfreter's (8) and Moscona's (10) pioneering work, cellular self-sorting has been widely recognized as a model for tissue formation (11, 14, 12) and even malignant invasion (6).

Methods

Cell culture

3T3_x cells were a spontaneous variant derived from normal Swiss 3T3 cells (a gift of Dr. Howard Green, Harvard Medical School) when grown in DME with 10 % fetal calf serum for passage numbers exceeding 40. Subsequently, the cells were split 1:3 and grown in DME with 10% of normal calf serum indefinitely. When confluent, the cells formed a reticular pattern of small colonies connected by strands of cells. In addition they turned the culture medium slightly yellow (pH = 6.8) suggesting that they expressed increased glycolysis. Normal 3T3 cells and CV-1 cells were grown under the same conditions as 3T3_x cells. BHK-21 cells were grown in DME supplemented with 10% calf serum and 10% tryptose phosphate broth.

Particles and particle suspensions

Latex particles were purchased from Polysciences, Inc. Warrington, PA. Diamond particles (Polycrystalline 1.00μm #SSX 0.75-1.25), called 'dark diamond' in the following, were purchased from L. M. Van Moppes, Geneva, Switzerland. A second kind of diamond particles (PCD-F 0-2μ), called 'white diamond' in the following, were purchased from Engis Co. Wheeling, IL 60090-9046. All particles were kept in an aqueous suspension of 2.5% solids. The suspension of diamond particles was sonicated before every use.

Preparation of hyper-scattering cells

Volumes between 20 [μl] and 200 [μl] of the particle suspensions were added to 8 [ml] of culture medium in 10 [cm] culture dishes. Three-day-old 3T3_x cells were trypsinized, and 2×10^6 cells were added to the particle-containing dish. After 2-3 day the particle-loaded cells were harvested by trypsinization, pelleted in a tabletop centrifuge, and re-suspended in normal culture medium by vigorous pipetting.

Measurement of light scattering of hyper-scattering cells

Samples of the cell suspensions used in the experiments were diluted to final concentrations of 2×10^5 [cells/ml], placed in cuvettes and irradiated from the side with the beam of GaAlAs laser (40 [mW]; 830 [nm]; GALA Laser System, D.O.Industries, Rochester, NY 14623)). At right angles to the beam a fiber optics cable fed the scattered light into a photomultiplier setup (Hamamatsu Photonics, Bridgewater, NJ 08807; Photomultiplier tube: R943-2; Socket: E 2762-506; Thermoelectric cooler: C4877-01; High voltage power supply: C3350) whose current was read on an oscilloscope.

Test substrates for uni-directional aggregation

The bottom of a 6 [cm] culture dish was coated with a 1-2 mm thin layer of Sylgard®184 (Dow Corning Corporation, Midland, MI 48686) and polymerized for 1 h at 55 °C generating a sterile surface that was entirely non-adhesive for cells. Subsequently, the surface was rendered partially adhesive by the vacuum evaporation of a thin, transparent film (approx. 50% light extinction) of NiCr (see 2) except in areas that were masked by 5 electron microscope grids (diameter: 3 [mm]) placed randomly on the Sylgard®184 surface prior to the evaporation. The copper electron microscope grids (EMS, Port Washington, PA 19034; # G300P-Cu) had a parallel bar pattern to produce parallel strips of alternating adhesive and non-adhesive areas. For the

experiments approximately 1.5×10^6 particle-containing cells were plated into 6 [ml] of culture medium of the test substrates which were fixed and examined 2 days later.

Results

Hyper-scattering cells

Based on darkfield microscopy the main light scattering objects of normal 3T3_x cells appeared to be their perinuclear granules such as lysosomes, mitochondria, peroxisomes, and phagosomes (Figure 1a; cell '1'). The ingested particles of particle-loaded 3T3_x cells accumulated around the nucleus like perinuclear particles. However, they scattered much more light than these (Figure 1a, cell 2; Figure 1b, cell '4') and remained inside the cells for several days. In the following, the particle loaded 3T3_x cells will be called 'hyper-scattering cells'.

The intensity of light scattering I_{sc} of such cells depended on the material, size and concentration of the ingested particles. Figure 2 shows the light scattering at 830 [nm] of hyper-scattering cells that had ingested different amounts and kinds of particles. The materials used were latex (Fig. 2 '1', '2') and synthetic diamond which appeared either 'dark gray' (Fig. 2 '3') or 'white' (Fig. 2 '4') depending on their method of catalysis. The conditions of the measurements are described in the Method section and were selected to generate a photomultiplier reading of 100 [mV] for the natural scattering of particle-free 3T3_x cells. The Figure indicates that the hyper-scattering cells exceeded the light scattering of 3T3_x cells in an adjustable way by as much as 175-fold.

The intensity of light scattering I_{sc} depended on particle size in a non-monotonous way (Fig. 5, '1'). The decrease of light scattering by hyper-scattering cells at particle diameters larger than 2 [μ m] (Fig. 2a) was due to a decreased uptake of larger particles by the cells.

Time lapse observations of the ingested particles demonstrated their incessant motion indistinguishable from that of normal perinuclear particles. This motion caused stochastic clustering of the particles which, in turn, generated continuous fluctuations of the scattered light.

Assay for uni-directional aggregation.

The test required a new assay to measure the distances between small aggregates of cultured cells in an unambiguous way. Its main feature was to restrict the cells to an essentially one-dimensional space (Figure 3). The assay used an array of parallel adhesive strips on an otherwise non-adhesive substrate whose ends formed a circle with radius $R = 1.25$ [mm] (Fig. 3a).

As shown in the Appendix, if cells were capable of aggregation on such an array their outermost aggregates would be located along a circular arc with the same radius R as indicated in Figure 3b. However, the arcs would be shifted by a distance of R_a towards the center of the array, where $2R_a$ is the average distance between cell aggregates. The value of R_a expresses how distant, on average, the initial locations of cells were from the aggregate that they formed ('range of aggregation').

Indeed, when plated hyper-scattering cells on such substrates they aggregated along the predicted circular arcs (Fig. 3c). Furthermore, as explained in the Appendix other clusters along the inside of the strips were located at about twice that distance from each other.

Time lapse observations showed that the first aggregates formed within 5 [h]. Some of them were capable of translocation as a whole away from the ends of the strips while individual cells migrated towards them. Cells that had accidentally landed on the non-adhesive areas between the adhesive strips extended pseudopodia and moved to the closest adhesive strip. Once fully spread many of the cells reached across the non-adhesive gaps and formed permanent bridges.

The method offered an easy, yet accurate measurement of the value of R_a . Since the radius R of the circular aggregation arcs is known, one can easily find the optimal fit of the array of clusters to 2 circles with this radius and measure the distance $d = 2R_a$ between them (Fig. 3d). The 2 circles have to intersect at the poles of the circular pattern of adhesive strips, which serves as an internal control for the curve fitting procedure. A particular advantage of the method is its independence from the hard to control plating densities of cells. These affected the optical densities of the aggregation arcs but not the location and geometric properties that are the basis of the method.

Image averaging

The precise circular geometry of the field of adhesive strips and of the aggregation arcs offered a simple averaging procedure to enhance the visibility of the aggregation arcs and, thus, the accuracy of the data (Fig. 4).

After orienting the adhesive strips of the original image (Fig. 4a) in a horizontal direction the image was superimposed on its own mirror image (Fig. 4b) resulting in a first level of enhancement of the visibility of any aggregation arcs. Throughout this article such mirrored images were used to determine the values of R_a . Applying this procedure to all 5 test fields of a test substrate yielded a standard deviation of approximately 12%.

For even better visibility one could carry the optical averaging further by superimposing each of the mirrored images of the 5 test fields of a test substrate. The procedure was equivalent to the optical average of $2 \times 5 = 10$ independent experiments (Fig. 4c).

Applying these methods yielded an average range of aggregation $R_a = 165 \text{ } [\mu\text{m}]$ (std.dev.= $30 \text{ } [\mu\text{m}]$) for $3\text{T}3_x$ -derived hyper-scattering cells. Pooling 100 values of R_a regardless of the experimental circumstances yielded values ranging between 83 and 247 $[\mu\text{m}]$.

Relationship between light scattering and range of aggregation.

The scattering intensity of hyper-scattering cells did not rise monotonously with the size of their ingested particles but decreased after reaching a peak for 2 $[\mu\text{m}]$ large particles (Figure 2a). As shown in Figure 5a the value of R_a changed in a similar way as a function of particle size, suggesting that light scattering may play a role in the range of aggregation.

The result posed the question whether the formation of aggregation arcs was related to my earlier experiments where particle-free $3\text{T}3$ cells were able to detect artificial near-infrared light sources up to a distance of 60-100 $[\mu\text{m}]$ (1). Since the visibility of the aggregation arcs depended on the visibility of the ingested particles in the microscope, one cannot determine directly the value of R_a for particle-free cells. However, one may use the results shown in Figure 5 to extrapolate to the case of particle size = 0 to obtain an approximate value of $R_a = 100 \text{ } [\mu\text{m}]$ for particle-free cells. This value of R_a agrees with the earlier, independent data.

Stronger evidence for a role of light in aggregation came from experiments that irradiated the hyper-scattering cells with different wavelengths of light. My earlier work (1, 2, 4) had suggested that $3\text{T}3$ cells reacted most sensitively to near-infrared light around 800 $[\text{nm}]$ if the light source pulsed. Therefore, the aggregation of hyper-scattering cells was tested that were irradiated continuously with the visible wavelength of 600 $[\text{nm}]$ or the near-infrared wavelength of 800 $[\text{nm}]$ light at intensities of 12-15 $[\mu\text{W}/\text{cm}^2]$ perpendicular to the surface of the test substrates. To be sure, the intensity of the artificial light sources in these experiments was not pulsating. However, as mentioned above, the light scattered by the stochastically moving perinuclear particles inside the cells was always fluctuating, nevertheless.

The averages of 3 independent experiments and 14 measurements for each data point showed a reduction $18 \pm 5\%$ of the value of R_a with visible light, whereas irradiation with the near-infrared wavelength increased the value of R_a by $14 \pm 4\%$ (Figure 6).

Perhaps the strongest support for a link between the light scattering I_{sc} of hyper-scattering cells and their range of aggregation R_a came from a plot of one versus the other. The plot used 5 logarithmically equal intervals of the light scattering intensities I_{sc} and sorted the values of R_a into these intervals accordingly. The value for particle-free $3\text{T}3_x$ cells was extrapolated from Fig. 5 and entered into the plot as the smallest value of scattering intensity. Figure 7 shows the averages of R_a for each of the sorting intervals. It appeared that the range of aggregation R_a almost doubled as the scattering intensity of the cells increased 18-20 fold over the value of particle-free cells. Surprisingly, at even higher scattering intensities $I_{sc} > 2000 \text{ } [\text{mV}]$, the range of aggregation decreased again. Concomitantly, in these cases the aggregation arcs seemed to form faster, as they became detectable already after 1 day of incubation, which may explain the decrease of R_a (See Discussion).

The 'range of aggregation' of other cell types

Not only $3\text{T}3_x$ cells but also other fibroblastic cell types such as normal $3\text{T}3$ cells and BHK cells formed aggregation arcs after their conversion to hyper-scattering cells. However it took normal $3\text{T}3$ cells and BHK cells 2-3 times longer than $3\text{T}3_x$ cells. As to their range of aggregation, the value of R_a for normal $3\text{T}3$ cells was the same as for $3\text{T}3_x$ cells. BHK hamster fibroblasts cells formed long stretched clusters and generated 28% larger values of R_a than $3\text{T}3$ cells (Fig. 8; white arrows in left-hand panel). On the other hand, an epithelial cell line, CV-1, formed poorly visible aggregation arcs, because the cells retained only very small clusters of phagocytosed particles. They also required 5-6 days to form. Yet, many clusters could be seen at

the very edge of the adhesive stripes yielding a value of $R_a = 0$ consistent with their epithelial character (Fig. 8; white arrows in right-hand panel). Most notably, they formed long chains of cells that bridged across the non-adhesive areas of the test substrates (not shown in Fig. 8).

Discussion

At first sight the changes of R_a reported here may appear small. It should be noted, though, that a one-dimensional increase of R_a as small as 26% would effectively double the volume from which a 3-dimensional cluster recruits its constituent cells, because $(1.26)^3 = 2$.

The ingested particles changed the aggregation behavior of the 3T3_x cells thus posing the central question of this article. Was the change of behavior due to the increased light scattering or to some other consequence of particle ingestion?

It is difficult to see which other consequence that might be. At present there is no mechanism to explain how the phagocytosis of particles could have induced the kinds of genetic, structural or functional changes that we usually associate with changes of cell behavior. After all, phagocytosis is a normal and frequent process in the life of all nucleated animal cells, and all the ingested particles were chemically inert.

Regardless, one may construct a hypothetical mechanism that changes the cell-to-substrate and cell-to-cell adhesion of cells depending on the size, amount and material of the ingested, inert particles. Based on this hypothesis one could then try to explain the observed changes of aggregation as a function of phagocytosis-induced changes of these two kinds of adhesion. Unfortunately, the complexity and deformability of cell shape have so far defeated every attempt to find quantitative assays for them, no matter how conceptually obvious they may appear. Therefore, such hypothetical mechanisms can neither be experimentally verified nor falsified and must remain a matter of intuition.

Admittedly, neither is there a mechanism to explain how light scattering could have accomplished these changes. However, my earlier work (1, 2, 3, 4) together with the results of the present article make it quite likely that it exists. Specifically, the present finding that the range of aggregation R_a can be increased by near-infrared light irradiation may be interpreted as an extension of the 'range of vision' of the cells. Likewise, the reduction of R_a by visible light may be interpreted as a partial 'blinding' of the cells.

Most telling, perhaps, was the direct relationship between the range of aggregation R_a and the intensity I_{sc} of the near-infrared light scattering of the cells (Fig. 7). It may suggest that the more the cells scatter light, the better they can be detected by distant others and, thus, the larger will be the distance from which they flock together. More specifically, the range of aggregation rose with the intensity of light scattering of the cells until it reaches a peak at around $I_{sc} = 2000$ [mV]. At higher intensities the range of aggregation shortens again while the aggregation arcs seemed to form faster.

The latter observation may offer an explanation for the surprising decline of R_a at very high scattering intensities. The faster speed of aggregate initiation may cause the number of aggregates to go up. As a result their average distance and size would decrease and, thus, the value of R_a . Alternatively, it seems possible that the large number of perinuclear particles inside cells with such high scattering intensities blocks the reception of the scattered light of other cells. Consequently, the cells would aggregate as if the other cells around would scatter less light than they actually do.

As mentioned in the Introduction, modern single photon detectors and sophisticated data-processing methods were barely able to detect the scattering of the black-body radiation by small groups of cells. If cells are able to detect such extremely small signals they, too, must employ a highly sophisticated detection and data-processing system that ultimately drives all the actions required for aggregation. Such actions would include adhesion, polarization, cytoskeletal architecture, shape changes, migration, interactions with the extracellular matrix and many more. Since several of these actions are also known to feed back on the genome (e.g. 7, 9, 13), the postulated data-processing systems appears capable of essentially controlling actions of the entire cell. Simply put, this mechanism would render cells 'intelligent' (5).

Appendix:

Uni-directional aggregation along thin strips of adhesive substrate places the first cell clusters at a fixed distance away from each end of a strip.

Assume that randomly plated cells are confined to an infinitely long, thin strip of adhesive substrate just wide enough to allow moving cells to pass each other (Fig. 9a). After the cells attach and spread on the adhesive strips they will migrate up and down the surface of the strips but not onto the non-adhesive surface surrounding the strips. If the cells are capable of aggregation then they will eventually form clusters at random locations with an average distance of $2R_a$ between them (Fig. 9c). Since the aggregating cells come together from the distance R_a on either side of a cluster, the distance R_a will be called the 'range of aggregation'. The midpoint 'w' at distances R_a between any 2 adjacent clusters may be considered a watershed of cell migration as the cells ahead of or behind this point effectively migrated to opposite direction as they formed clusters (Fig. 9d). Cutting the strip off at such a location (Fig. 9e) would not affect the clustering behind it because the cut-off cells ahead of the cut would have migrated to the opposite direction, anyway. Therefore, each first cluster is located at a distance of R_a from the end of the strip.

Acknowledgement

I am grateful to Dr. Howard Green (Harvard Medical School, Boston MA) and to Dr. Leonid Margolis (National Institutes of Health, Bethesda MD) for many valuable discussions and to Dr. Lester Binder (Northwestern University) for the use of his microscope and high-resolution digital camera. This work was supported by a pilot grant from DARPA (&&&) and the Air Force Office of Scientific Research (&&&). My special thanks goes to Comdr. Kurt Henry, MD (DARPA) and Hugh DeLong, Ph.D. (AFOSR) for their courageous support.

References

1. Albrecht-Buehler, G., Surface extensions of 3T3 cells towards distant infrared sources. *J. Cell Biol.* (1991)114:493-502
2. Albrecht-Buehler, G. A rudimentary form of cellular 'vision'(1992) *Proc. Natl. Acad. Sci. USA* 89:8288-8292
3. Albrecht-Buehler, G. Changes of cell behavior by near-infrared signals. *Cell Motility and the Cytoskeleton* 32:299-304 (1995).
4. Albrecht-Buehler, G., Altered Drug Resistance of Microtubules in Cells Exposed to Infrared Light Pulses: Are Microtubules the "Nerves" of Cells? (1998) *Cell Motility and the Cytoskeleton* 40:183-192
5. Albrecht-Buehler, G. Cell intelligence (1998) <http://www.basic.northwestern.edu/g-buehler/cellint0.htm>
6. Armstrong, P.B. and M. T. Armstrong. Intercellular invasion and the organizational stability of tissues: a role for fibronectin. (2000) *Biochimica et Biophysica Acta* 1470: O9-O20
7. Folkman, J. and A. Moscona (1978) Role of cell shape in growth control. *Nature* 273: 345-349
8. Holtfreter, J. Experimental studies on the development of the pronephros. (1944) *Rev.Can.Biol.* 3:220
9. Ingber DE, Folkman J. (1989) Mechanochemical switching between growth and differentiation during fibroblast growth factor-stimulated angiogenesis in vitro: role of extracellular matrix. *J. Cell Biol.* 109:317-330.
10. Moscona, A. and H. Moscona (1952) The dissociation and aggregation of cells from organ rudiments of the early chick embryo. *J.Anat.* 86:287
11. Moscona A.A. (1960) Patterns and mechanisms of tissue reconstruction from dissociated cells. In *Developing Cell Systems and Their Control*, Ed. Rudnick, D. Academic Press, New York, pp 45
12. Steinberg, M. S. (1963) Reconstruction of tissues by dissociated cells. *Science* 141:401-408
13. Streuli CH, Bailey N and Bissell MJ. (1991) Control of mammary epithelial differentiation: Basement membrane induces tissue-specific gene expression in the absence of cell-cell interaction and morphological polarity. *J Cell Biol.* 115:1383-95.
14. Townes, P. and J. Holtfreter (1955) Directed movements and selective adhesion of embryonic amphibian cells. *J.Exp.Zool.* 128:53

Figure Legends

Figure 1. Darkfield micrographs of normal and hyper-scattering cell. The nuclei of selected cells are marked with numbers 1-4.

- a: The perinuclear granules (png) of normal 3T3_x cells ('1') scatter much less light than the ingested 1 μ m large latex particles of a hyper-scattering cell ('2').
- b: The ingested 1 μ m large latex particles of a hyper-scattering cell ('3') scatter much less than the 1 μ m large dark diamond particles of another hyper-scattering cell ('4').
- c: Fluorescence micrograph of the same field as panel b demonstrating the presence of the fluorescent labeled latex particles of cell '3'.

Figure 2. Standardized light scattering I_{sc} of hyper-scattering cells at 830 [nm] as a function of the concentration (w/w) of particles of different materials. (For conditions of the standardization see text).

- (1): 1 [μ m] large latex particles. (2): 2 [μ m] large latex particles. (3): 1 [μ m] large dark diamond particles. (4): 1 [μ m] large white diamond particles .

Figure 3. Assay for uni-directional aggregation (bar in panel a indicates 1 mm).

- a: Circular pattern of adhesive strips (gray areas) on a non-adhesive substrate (bright areas) generated by evaporating a thin layer of NiCr onto a Sylgard®184 surface using a bar pattern electron microscope grid as mask (radius of circle $R = 1.25$ [mm]).
- b: Expected location of the first cell clusters along 2 circular arcs near the end of each strip provided the cells aggregate (see Appendix). Each is shifted by R_a ('range of aggregation') from the edge of the circle ($2R_a$ = average distance between cell clusters).
- c: Example of aggregates of hyper-scattering cells located along the predicted aggregation arcs as seen in bright-field microscopy.
- d: Quantitative evaluation of the circular aggregation arcs by matching them to 2 circles of radius R . The shift between the circles is equal to $2R_a$.

Fig. 4. Increase of visibility and accuracy of the aggregation arcs by image averaging. a: unprocessed image. b: superimposing of the image with its own mirror image. c: Image average of all 5 test fields of a test substrate each processed as in (b).

Figure 5. Parallels between the intensity of light scattering I_{sc} of hyper-scattering cells at 830 [nm] (right-hand ordinate) and the range of aggregation R_a (left-hand ordinate) of the same cells as non-monotonous functions of particle size (abscissa). (particle concentration: $1.5 \times 10^{-2}\%$; 2 independent experiments; 10 measurements for each data point).

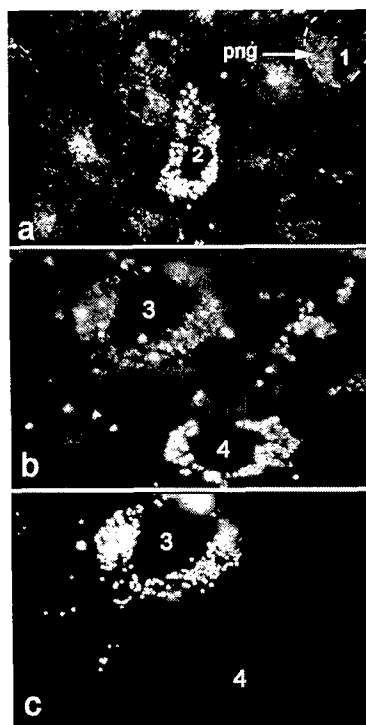
Figure 6. Effect of continuous irradiation of the cells with $12-15$ [μ W/cm²] at a distance of 45 [mm]. The columns represent the average of 14 measurements in 3 independent experiments. Error bars indicate the error of the mean.

Figure 7. Relationship between the scattered intensity I_{sc} of hyper-scattering cells and their average range of aggregation R_a . Each data point represents the average of 17-28 individual measurements of R_a . Horizontal error bars indicate the size of the sorting intervals that yielded the indicated averages. Vertical error bars indicate the error of the mean of these averages.

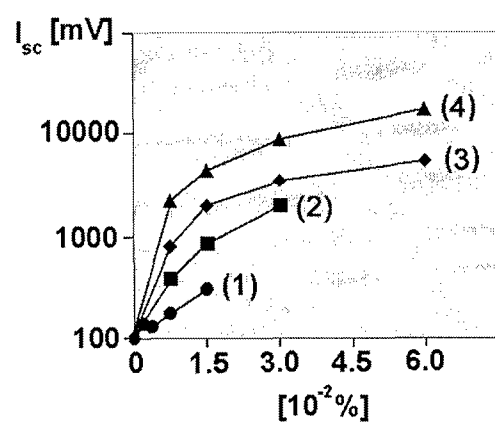
Figure 8. Aggregation arcs formed by other cell types. The images are superimposed on their mirror images. White arrows point to some of the clusters.

Figure 9. Schematic of uni-directional aggregation (explanation see text)

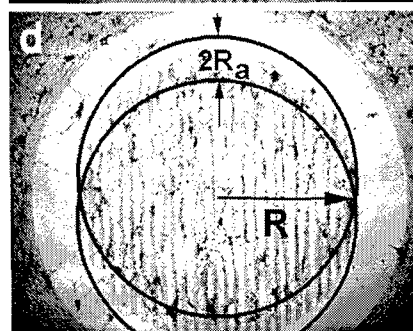
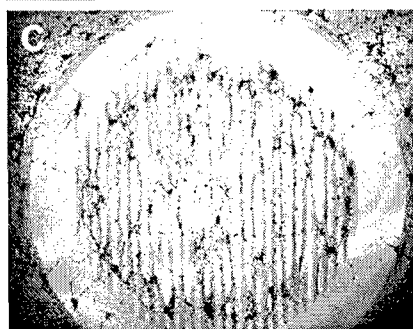
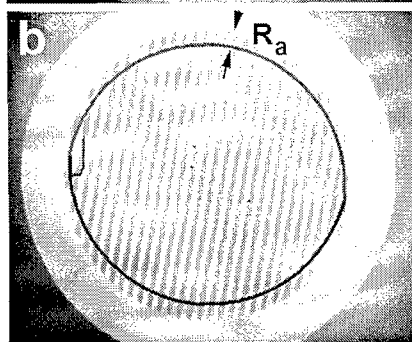
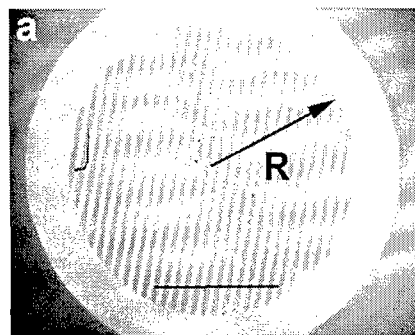
(1)



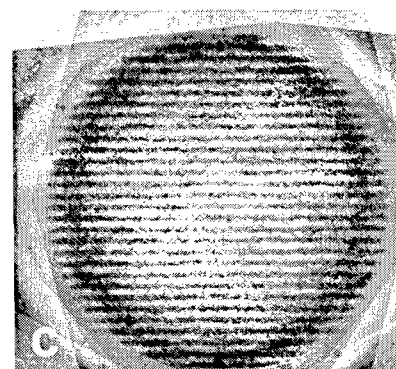
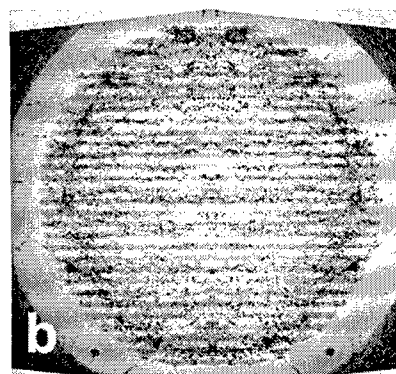
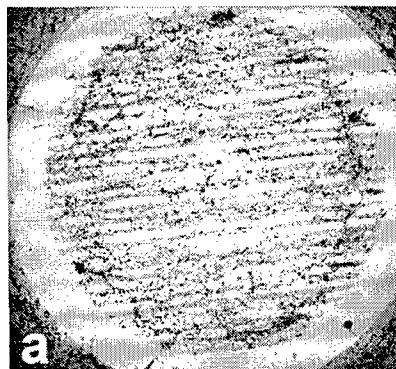
(2)



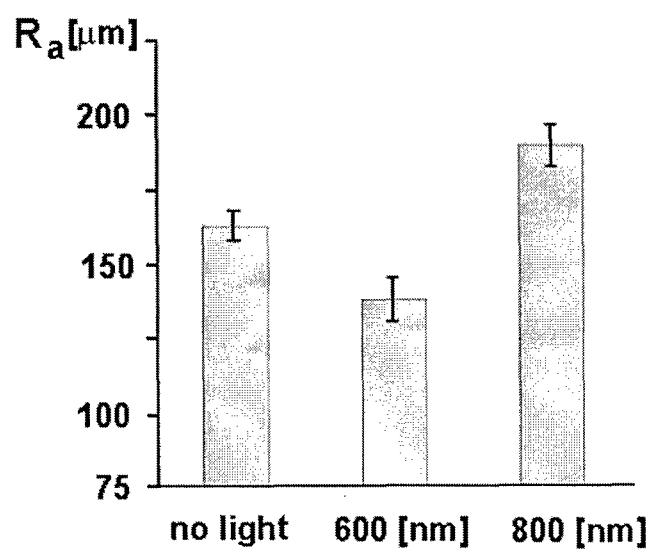
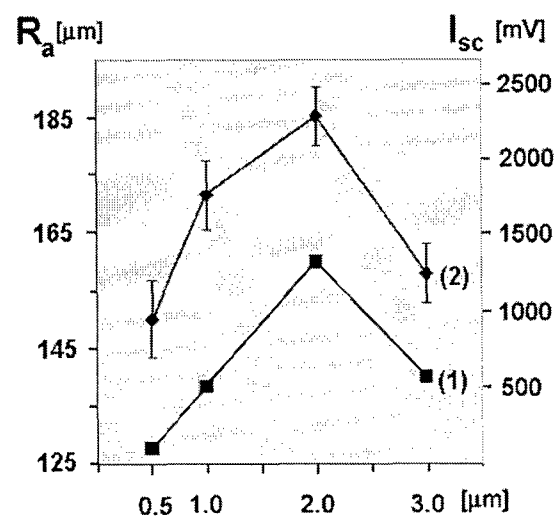
(3)



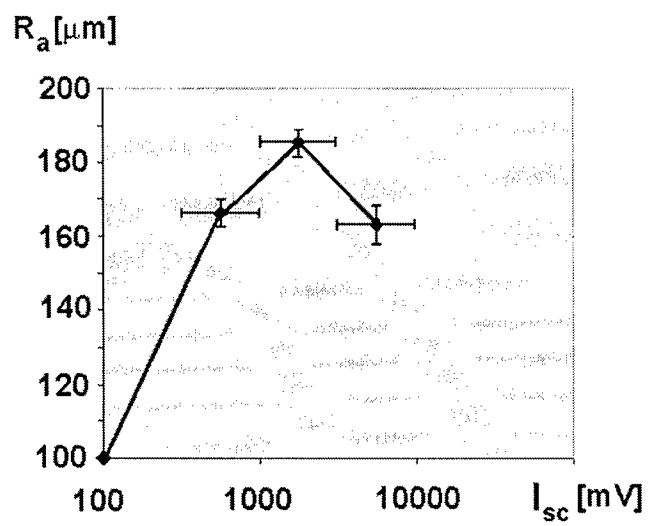
(4)



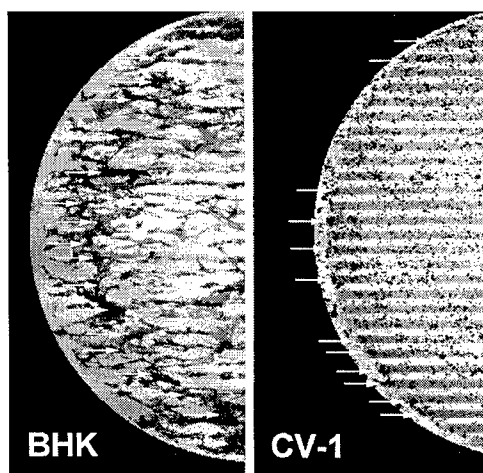
(5)



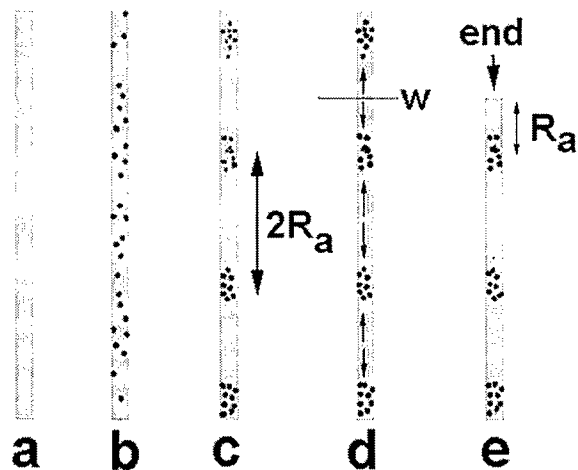
(6)



(7)



(8)



(7)

Future Outlook.

Once we know that light scattering by cells is the mechanisms they use to interact at large distances, we can begin to record their light scattering at near-infrared wavelengths at medically important events, such as development, wound healing, metastasis etc. Subsequently, we can play back these recordings in order to influence cell behavior in very specific ways.

9. INTERACTIONS/TRANSITIONS

a. Participation at meetings where aspects of the work were presented

Third International Conference on Tumor Metabolism. 10/20-10/22/2005,
Louisville, KY

b. Transitions

Cooperation with DARPA projects PIC and ReGenesis.

10. Honors/Awards

2002 Member, European Academy of Sciences, Brussels
2003 Fellow, European Academy of Sciences, Brussels